MAXIMUM LIKELIHOOD SHIFT ESTIMATION USING HIGH RESOLUTION POLARIMETRIC SAR CLUTTER MODEL

Olivier Harant[1,2]**, Lionel Bombrun**[2]**, Gabriel Vasile**[1]**, Laurent Ferro-Famil**[3]**, Michel Gay**[1]

[1] *Grenoble-Image-sPeech-Signal-Automatics Lab*
GIPSA-lab DIS/SIGMAPHY, CNRS
Grenoble INP, 961 rue de la Houille Blanche, BP 46 38402 Grenoble, France
{olivier.harant|gabriel.vasile|michel.gay}@gipsa-lab.grenoble-inp.fr

[2] *Université de Bordeaux, UB1, IPB, ENSEIRB-Matmeca, Laboratoire IMS*
UMR 5218, Groupe Signal et Image, Talence, France
lionel.bombrun@ims-bordeaux.fr

[3] *Institute of Electronics and Telecommunications Rennes*
IETR SAPHIR, CNRS
Université de Rennes 1, Bat. 11D, 263 avenue du Général Leclerc 35042 Rennes, France
Laurent.Ferro-Famil@univ-rennes1.fr

ABSTRACT

This paper deals with a Maximum Likelihood (ML) shift estimation method in the context of High Resolution (HR) Polarimetric SAR (PolSAR) clutter. Texture modeling is exposed and the generalized ML texture tracking method is extended to the merging of various sensors. Some results on displacement estimation on the Argentière glacier in the Mont Blanc massif using dual-pol TerraSAR-X (TSX) and quad-pol RADARSAT-2 (RS2) sensors are finally discussed.

Key words: Polarimetric SAR, Texture modeling, ML tracking, sensor merging, glacier.

1. INTRODUCTION

Glacier monitoring has always been of importance. It is essential to follow their stability in order to limit some natural risks like serac avalanche. Moreover the velocity fields on the glaciers surfaces are useful for modeling their flow. Due to all weather capabilities, SAR sensors offer some powerful tools to fulfilling this task. This paper deals with a ML shift estimator method with sensors merging applied to displacement estimation of the glaciers surfaces.
This generalised ML shift estimator takes into account the specificity of the new generation of airborne and spaceborne SAR sensors which have indeed less scatterers in each resolution cell. The homogeneous hypothesis of the Polarimetric SAR clutter may be reconsidered and heterogeneous clutter models have therefore recently been studied with POLSAR data through the SIRV processes [7].
In polarimetric case, the target vector $\mathbf{k}$ can be decomposed as the product of a square root of a positive random variable τ (representing the texture) with an independent complex Gaussian vector $\mathbf{z}$ with zero mean and covariance matrix $[M] = E\{\mathbf{z}\mathbf{z}^H\}$ (representing the speckle): $\mathbf{k} = \sqrt{\tau}\ \mathbf{z}$, where the superscript H denotes the complex conjugate transposition and $E\{\cdot\}$ the mathematical expectation.

To fully exploit the variety of HR SAR sensors, authors propose to enlarge the shift estimator based on this SIRV decomposition with the merging of HR PolSAR sensors. After having reminded the general ML texture tracking method, the benefit of the modeling the texture τ with a Fisher Probability Density Function (PDF) is exposed and similarity criteria for both uncorrelated and correlated texture are defined. The last section focuses on the merging of HR PolSAR sensors. The merging principle is introduced and finally some preliminary results are discussed.

2. ML TEXTURE TRACKING

The texture parameter τ contains the main information for shift estimation applications. This section details the general method using one sensor. Then the extracted texture modeling is discussed to finally define the similarity criteria in both uncorrelated and correlated texture cases.

Let consider a Master/Slave pair of blocks of the PolSAR data-set containing n pixels, respectively $\mathbf{k}_y^i =$

$\left[\mathbf{k}_{y_1}^i, \ldots, \mathbf{k}_{y_n}^i\right]$ and $\mathbf{k}_x = [\mathbf{k}_{x_1}, \ldots, \mathbf{k}_{x_n}]$. The texture blocks $\tau_y^i = \left[\tau_{y_1}^i, \ldots, \tau_{y_n}^i\right]$ and $\tau_x = [\tau_{x_1}, \ldots, \tau_{x_n}]$ are estimated according to the following SIRV scheme. The slave block i is shifted from the master one with a displacement $\overrightarrow{v}_i$ as it is illustrated in Fig. 2. In this section, the vector $\overrightarrow{v}_i$ is limited to a translation and has only two components $[{v_i}^d, v_i^{az}]$ in range and azimuth. The ML texture tracking algorithm estimates the shift vector $\overrightarrow{v}_{\text{ML}}$ by maximizing for each slave block i the Conditional Density Function (CDF) [3]. It yields:

$$\overrightarrow{v}_{\text{ML}} = \underset{i}{\text{Argmax}}\ p\left(\tau_x | \tau_y^i, \overrightarrow{v}_i\right). \tag{1}$$

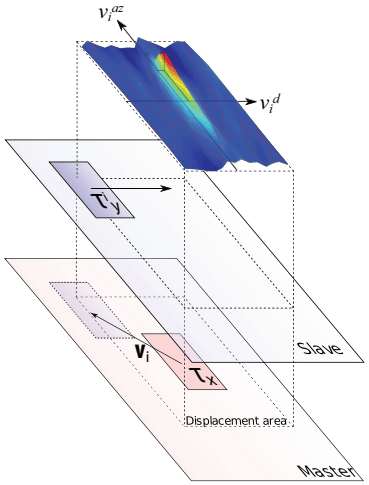

Figure 1. Shift estimation general principle

The global scheme of this method may be decomposed as follows:

- Texture estimation using SIRV model (subsection 2.1).
- Texture modeling (subsection 2.2).
- Similarity criteria derivation for both uncorrelated and correlated texture cases (subsection 2.3).

The following subsection introduces how to estimate τ from HR PolSAR data using SIRV model.

2.1. SIRV estimation scheme

For a given covariance matrix $[M]$, the ML estimator of the texture parameter τ for the pixel i ($\hat{\tau}_i$) is given by:

$$\hat{\tau}_i = \frac{\mathbf{k}_i^H [M]^{-1} \mathbf{k}_i}{p}, \tag{2}$$

where p is the dimension of the target scattering vector $\mathbf{k}$ ($p = 3$ in the reciprocal case).

Under the deterministic texture case, the ML estimator of the normalized covariance matrix is the solution of the following recursive equation:

$$\begin{aligned}[\hat{M}_{ML}] = f([\hat{M}_{ML}]) &= \frac{p}{N} \sum_{i=1}^{N} \frac{\mathbf{k}_i \mathbf{k}_i^H}{\mathbf{k}_i^H [\hat{M}_{ML}]^{-1} \mathbf{k}_i} \\ &= \frac{p}{N} \sum_{i=1}^{N} \frac{\mathbf{z}_i \mathbf{z}_i^H}{\mathbf{z}_i^H [\hat{M}_{ML}]^{-1} \mathbf{z}_i}.\end{aligned} \tag{3}$$

In the random texture τ case, the ML estimator of the normalized covariance matrix depends on the texture Probability Density Function (PDF) $p_\tau(\tau)$ and is given by [2]:

$$[\hat{M}_{ML}] = \frac{1}{N} \sum_{i=1}^{N} \frac{h_{p+1}\left(\mathbf{k}_i^H [\hat{M}_{ML}]^{-1} \mathbf{k}_i\right)}{h_p\left(\mathbf{k}_i^H [\hat{M}_{ML}]^{-1} \mathbf{k}_i\right)} \mathbf{k}_i \mathbf{k}_i^H \tag{4}$$

where $h_p(x)$ is the density generator function defined by:

$$h_p(x) = \int_0^{+\infty} \frac{1}{\tau^p} \exp\left(-\frac{x}{\tau}\right) p_\tau(\tau)\, d\tau \tag{5}$$

Pascal *et al.* have established the existence and the uniqueness, up to a scalar factor, of the ML estimator of the normalized covariance matrix, as well as the convergence of the recursive algorithm whatever the initialization [6].
In usual cases, the texture τ is not deterministic but for sake of simplicity, this study is limited to the first ML estimator (3) which is approximate in our case.

It is important to notice that in the SIRV definition, the PDF of the texture random variable is not specified. As a consequence, SIRVs describe a whole class of stochastic processes. This class includes the conventional clutter models having Gaussian, $\mathcal{K}$, $\mathcal{G}^0$, KummerU PDFs which correspond respectively to Dirac, Gamma, Inverse Gamma and Fisher distributed texture [1].

2.2. Texture modeling

According to the general ML tracking method [4], the texture component τ must be firstly modeled. For a chosen area from any HR PolSAR image, the texture component τ and the intensity image cannot be modeled with the same PDFs as it is shown in Fig. 2. In this paper, the

Fisher PDF is used to model the texture parameter τ:

$$p_\tau(\tau) = \mathcal{F}[m, \mathcal{L}, \mathcal{M}] = \frac{\Gamma(\mathcal{L}+\mathcal{M})}{\Gamma(\mathcal{L})\Gamma(\mathcal{M})} \frac{\mathcal{L}}{\mathcal{M}m} \frac{\left(\frac{\mathcal{L}\tau}{\mathcal{M}m}\right)^{\mathbf{L}-1}}{\left(1+\frac{\mathcal{L}\tau}{\mathcal{M}m}\right)^{\mathbf{L}+\mathbf{M}}} \quad (6)$$

where m is a scale parameter, $\mathcal{L}$ and $\mathcal{M}$ are two shape parameters.

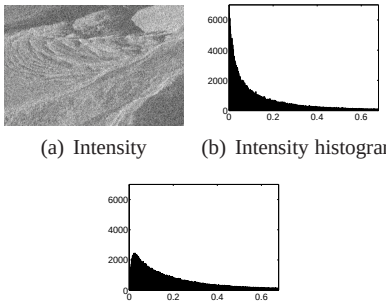

(a) Intensity (b) Intensity histogram

(c) Texture histogram

Figure 2. Histograms of a TSX -HH- channel sample (a) in intensity (b) and the texture τ component (c) image. TSX 2009-01-28 - Argentière glacier serac fall.

To highlight the benefit of this PDF for modeling HR texture component, the log-cumulant of order two end three, κ_2/κ_3 plan may be used. It is indeed representative of the Pearson family distributions like Fisher PDFs. This plan is divided into three distinct areas (Fig. 4(b)): the boundary between the Beta and Fisher domains represents the Gamma PDFs and that between the Fisher and Inverse Beta domains represents the Inverse Gamma PDFs.
Fig. 3 shows some κ_2/κ_3 plots estimated from Fig. 2(a) using various sliding window sizes. The convergence to Gamma PDFs is quite obvious in the case of the intensity image (Fig. 3(a)). The density of points in the tail of the cloud is negligible compared to that of the heart. Also the texture τ has a behavior which tends to converge to a Fisher PDF (Fig. 3(b)). Fig. 3(c) illustrates a simulated case where some log-cumulants estimations of Fisher PDF samples converge to the theoretical κ_2/κ_3 point.

From this κ_2/κ_3 representation, a basic classification of the kind of modeling may be computed on the image. Fig. 4(a) shows an example of such classification on the texture image extracted from the serac fall area of the Argentière glacier. The relevance of the Fisher modeling is checked almost everywhere.

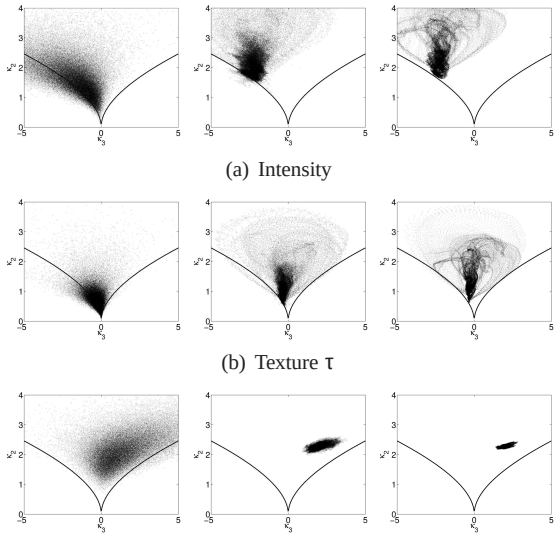

(a) Intensity

(b) Texture τ

(c) 500×500 pixels sampled from a Fisher PDF ($\mathcal{L} = 2$ $\mathcal{M} = 1$)

Figure 3. κ_2/κ_3 plan for various sliding window sizes computed on texture and intensity images of Fig. 2(a) and on a simulated Fisher distributed dataset. $N = [7 \times 7,\ 51 \times 51,\ 99 \times 99]$ is the sliding window size respectively from left to right.

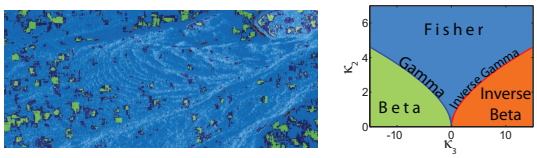

(a) Classification (b) κ_2/κ_3 plan

Figure 4. Modeling classification on texture image τ of the serac fall of the Argentière glacier. Log-cumulant estimation with a 19×19 pixels sliding window

2.3. Similarity criteria for uncorrelated and correlated texture

After having chosen a texture modeling, the ML tracking method needs to derive the texture ratio PDF p_α in both cases of correlated and uncorrelated texture between images.

2.3.1. Texture model with uncorrelated texture between images

For a Fisher distributed texture, authors have established the texture ratio PDF for uncorrelated texture between

images. Its expression is given by [5]:

$$p_\alpha(\alpha) = \frac{B(2\mathcal{L},2\mathcal{M})}{\left[B(\mathcal{L},\mathcal{M})\right]^2}\frac{1}{\alpha^{\mathbf{M}+1}} \times {}_2F_1\left(\mathcal{L}+\mathcal{M},2\mathcal{M};2\left(\mathcal{L}+\mathcal{M}\right);\frac{\alpha-1}{\alpha}\right) \quad (7)$$

where ${}_2F_1(\cdot,\cdot;\cdot;\cdot)$ and $B(\cdot,\cdot)$ are respectively the Gauss hypergeometric function and the Euler Beta function. Note that for uncorrelated texture between images, the scale parameter m simplifies when the texture ratio PDF is studied.

By combining (1) and (7), and following the same procedure as [3], the similarity measure is obtained [5]:

$$\begin{aligned}\mathrm{L}(\overrightarrow{v}_i) &= n\ln\left(\frac{B(2\mathcal{L},2\mathcal{M})}{\left[B(\mathcal{L},\mathcal{M})\right]^2}\right) \\ &- (\mathcal{M}+1)\sum_{j=1}^{n}\ln\tau_{x_j} + \mathcal{M}\sum_{j=1}^{n}\ln\tau_{y_j}^i \\ &+ \sum_{j=1}^{n}\ln\left({}_2F_1\left(\mathcal{L}+\mathcal{M},2\mathcal{M};2\left(\mathcal{L}+\mathcal{M}\right);1-\frac{\tau_{y_j}^i}{\tau_{x_j}}\right)\right).\end{aligned} \quad (8)$$

2.3.2. Texture model with correlated texture between images

The texture ratio PDF for correlated texture between images has been derived from the bivariate Fisher distribution. Its expression is given by [5]:

$$p_\alpha(\alpha) = \frac{R_1^{\mathbf{L}_1}\,R_2^{\mathbf{L}_2}\,B(\mathcal{L}_1+\mathcal{L}_2,\mathcal{M}_2)}{B(\mathcal{L}_1,\mathcal{M}_1)\,B(\mathcal{L}_2,\mathcal{L}_1+\mathcal{M}_2)} \times \frac{\alpha^{\mathbf{L}_1-1}}{(R_1\alpha+R_2)^{\mathbf{L}_1+\mathbf{L}_2}} \times {}_2F_1\left(a,b;c;z\right). \quad (9)$$

where $a = \mathcal{L}_1+\mathcal{L}_2$, $b = \mathcal{M}_2-\mathcal{M}_1$, $c = \mathcal{L}_1+\mathcal{M}_2$, $z = \dfrac{1}{1+\frac{R_2}{R_1}\frac{1}{\alpha}}$, $R_1 = \dfrac{\mathcal{L}_1}{\mathcal{M}_1 m_1}$ and $R_2 = \dfrac{\mathcal{L}_2}{\mathcal{M}_2 m_2}$.

Similarly, combining (1) and (9) yields to:

$$\begin{aligned}\mathrm{L}(\overrightarrow{v}_i) &= n\ln\left(\frac{B(\mathcal{L}_1+\mathcal{L}_2,\mathcal{M}_2)}{B(\mathcal{L}_1,\mathcal{M}_1)\,B(\mathcal{L}_2,\mathcal{L}_1+\mathcal{M}_2)}\right) \\ &+ n\mathcal{L}_1\ln R_1 + n\mathcal{L}_2\ln R_2 + (\mathcal{L}_1-1)\sum_{j=1}^{n}\ln\tau_{x_j} \\ &- \mathcal{L}_1\sum_{j=1}^{n}\ln\tau_{y_j}^i - (\mathcal{L}_1+\mathcal{L}_2)\sum_{j=1}^{n}\ln\left(R_1\frac{\tau_{x_j}}{\tau_{y_j}^i}+R_2\right) \\ &+ \sum_{j=1}^{n}\ln\left({}_2F_1\left(a,b;c;z\right)\right).\end{aligned} \quad (10)$$

These criteria definitions are at the heart of the ML tracking method and may be used with any texture component for any sensor. Moreover, the Fisher PDF tends to a Gamma PDF when $\mathcal{M}$ tends to infinity, hence this method works even if the homogeneous clutter hypothesis still valid.

3. SENSOR MERGING

Various HR SAR sensors are available and merging them in order to fully exploit their complementarity may be interresting.
Based on the previous "single sensor" method scheme, the next section deals with a step of sensors merging. A preliminary hypothesis is done: all images pairs are acquired at the same period. In case of glaciers monitoring application, the time offset between images pairs must be less than 13% of the acquisition time difference between the Master and Slave images. This tolerance is realistic because the variation of velocity within 13% is negligible.

3.1. Principle

A Digital Elevation Model (DEM) is used as common referential between both sensors and the velocity vector $\overrightarrow{v}_i$ is defined in this referential.
By analogy with the usual method, the shift vector in case of merged ML tracking may be formulated as follows:

$$\overrightarrow{v}_{\mathrm{ML}} = \underset{i}{\mathrm{Argmax}}\; p\left(\tau_{x_1},\cdots,\tau_{x_k}|\tau_{y_1}^i,\cdots,\tau_{y_k}^i,\overrightarrow{v}_i\right), \quad (11)$$

where k is the number of sensors.

First of all, it is necessary to compute each Look Up Table (LUT) to georeference each sensor to the DEM. In the context of the EFIDIR[1] project, "SARLut" tools has been developed to compute such LUTs from any georeferenced DEM to any SAR geometry.
The general principle of merging sensor is quite similar with the usual method [4] except that the sliding process is done on the DEM whereas the sliding windows are extracted on the SAR images. Finally, the similarity criteria computed from each sensor are summed according to the following equation:

$$\mathrm{L}_{ALL}(\overrightarrow{v}_i) = \sum_{j=1}^{k}\frac{1}{n_j}\mathrm{L}_j(\overrightarrow{v}_i), \quad (12)$$

where n_j is the number of pixels of the j^{th} sensor sliding windows and $\overrightarrow{v}_i$ is the ground velocity vector with two components $[v_i^{lat}, v_i^{lon}]$ respectively along latitude and

[1] www.efidir.fr

longitude.
The size of the sliding windows depends on the image resolution and is calculated to cover the same surface for each sensor. Hence n_j normalizes the likelihood functions values $\mathrm{L}_j(\overrightarrow{v}_i)$.

For one pixel X of the DEM, the merging principle may be written under the following pseudo-code:

for *each sensor* j **do**
  Find $\mathrm{LUT}_j(X)$ in the j^{th} sensor geometry.
  Extract τ_{x_j} around $\mathrm{LUT}_j(X)$.
end
for *each pixel* Y_i *of the DEM* **do**
  for *each sensor* j **do**
    Find $\mathrm{LUT}_j(Y_i)$ in the j^{th} sensor geometry.
    Extract $\tau^i_{y_j}$ around $\mathrm{LUT}_j(Y_i)$.
    Compute $\mathrm{L}_j(\overrightarrow{v}_i)$ with (8) or (10).
  end
  Compute $\mathrm{L}_{ALL}(\overrightarrow{v}_i)$ with (12).
end
$\overrightarrow{v}_{\mathrm{ML}}(X) = \underset{i}{\mathrm{Argmax}}\ \mathrm{L}_{ALL}(\overrightarrow{v}_i)$.

Algorithm 1: Pseudo-code of merging process for ML tex ture tracking for a pixel X of the DEM.

The merging principle is illustrated in Fig. 5 in the case of two sensors.

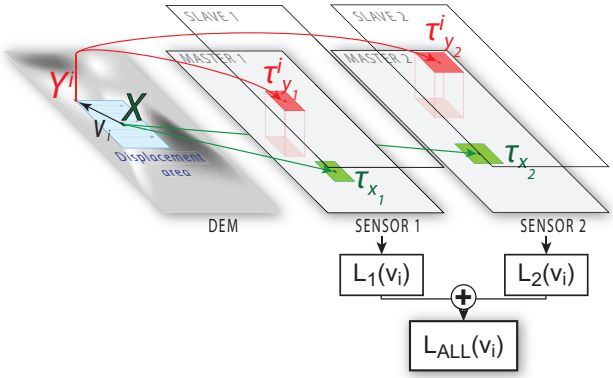

Figure 5. ML tracking with sensor merging principle

3.2. Results

Preliminary results are presented using HR SAR images acquired at the same period: one 24 days separated images pair of C band quad-pol RS2 (2009/01/29 and 2009/02/22) and one 22 days separated images pair of X band dual pol TSX (2009/01/28 and 2009/02/19).
To analyze the benefit of merging sensors, some averages of detection surfaces issued from this ML tracking process have been computed along the velocity vector components $(v^{lat}_{ML}, v^{lon}_{ML})$. Some of these surfaces have been plotted in Fig. 6. Four cases have been studied: similarity criterion on RS2, TSX, both sensors and cross-correlation criterion on TSX. These four selected cases highlight various behaviors of the merging process. Below each surface, a quality factor Q qualifies the "sharpness" of the peak and is defined as follows [3]:

$$Q = \frac{\max_i(\mathrm{L}(\overrightarrow{v}_i)) - \mathrm{mean}_i(\mathrm{L}(\overrightarrow{v}_i))}{\mathrm{mean}_i(\mathrm{L}(\overrightarrow{v}_i)) - \min_i(\mathrm{L}(\overrightarrow{v}_i))}. \qquad (13)$$

Fig 6(a) represents the average of detection surfaces for a null velocity $(v^{lat}_{ML}, v^{lon}_{ML}) = (0, 0)$. In that case all the criteria are robust because the no-motion texture is usually stable in time (banks of the glacier). In the second case (Fig 6(b)), both RS2 and TSX detection surfaces are noisy whereas the merged detection surface is sharp. Finally the last two subfigure highlight the robustness of the merged criterion as it follows the same behavior as the best individual case. For instance in 6(d) the quality of the RS2 criterion is weak whereas the merged criterion keeps the TSX criterion behavior.

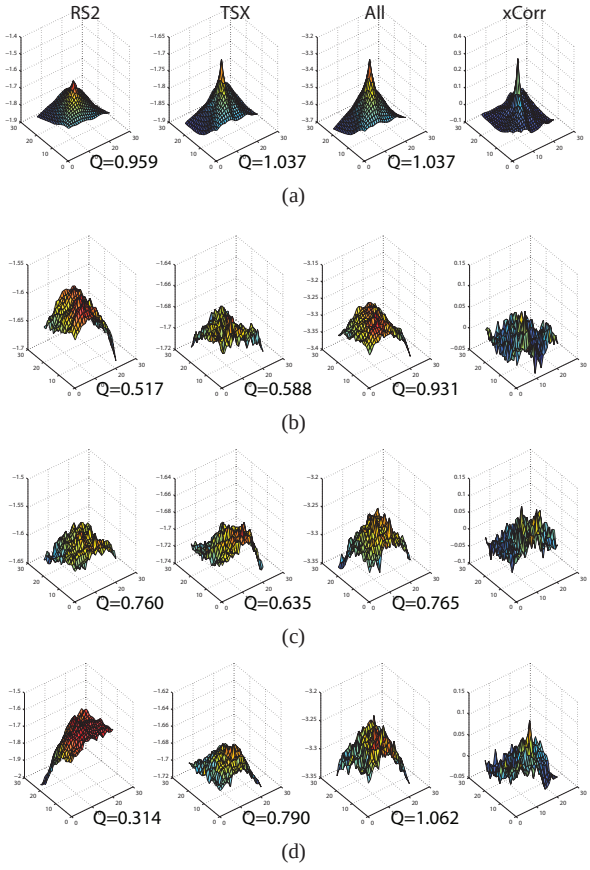

Figure 6. Several detection surfaces computed from RS2, TSX, both sensors and normalized cross-correlation on TSX, respectively left to right.

4. CONCLUSION

This paper highlighted the potential of combining acquisition in order to generalize the ML tracking method to a multi-temporal and multi-frequency texture tracking. The benefit of the Fisher PDF for texture modeling has been detailed and validated through a basic modeling classification on a texture image extracted from the Argentière glacier. After having defined the similarity criteria based on Fisher modeling, the ML texture tracking algorithm has been extended to the merging of sensors whose complementarity has been underlined in case of TSX and RS2 sensors.
Further works will be focused on the generalization of the merging process by removing the acquisition synchronization constraint. On the other hand, single pair shift estimator may be developed for using mixed frequency pair of images (i.e. one Master X band and one Slave C band). Moreover the georeferenced tracking makes easier the comparison with ground truth because the shift vector is directly obtained on the DEM.

ACKNOWLEDGEMENT

This work is supported by the French Research Agency (ANR) through the EFIDIR project (ANR-2007-MCDC0-04, http://www.efidir.fr) and the GlaRiskALP project. The authors wish also to thank the Rhône Alpes region, DIACT MEEDDAT and the other partners (SIVOM, St Gervais town, CG73, CG74, PACA).

REFERENCES

[1] L. Bombrun and J.-M. Beaulieu. Fisher Distribution for Texture Modeling of Polarimetric SAR Data. *IEEE Geoscience and Remote Sensing Letters*, 5(3), July 2008.

[2] L. Bombrun, G. Vasile, M. Gay, and F. Totir. Hierarchical Segmentation of Polarimetric SAR Images Using Heterogeneous Clutter Models. *IEEE Transactions on Geoscience and Remote Sensing*, 2010.

[3] E. Erten, A. Reigber, O. Hellwich, and P. Prats. Glacier Velocity Monitoring by Maximum Likelihood Texture Tracking. *IEEE Transactions on Geoscience and Remote Sensing*, 47(2):394–405, 2009.

[4] O. Harant, L. Bombrun, G. Vasile, L. Ferro-Famil, R. Fallourd, M. Gay, E. Trouvé, J.M. Nicolas, and F. Tupin. Fisher pdf for maximum likelihood texture tracking with high resolution polsar data. In *8th European Conference on Synthetic Aperture Radar, EUSAR '10*, 2010.

[5] O. Harant, L. Bombrun, G. Vasile, M. Gay, and L. Ferro-Famil. Maximum likelihood texture tracking in highly heterogeneous polsar clutter. In *IGARSS*, 2010.

[6] F. Pascal, Y. Chitour, J. P. Ovarlez, P. Forster, and P. Larzabal. Covariance Structure Maximum-Likelihood Estimates in Compound Gaussian Noise : Existence and Algorithm Analysis. *IEEE Transactions on Signal Processing*, 56(1):34–48, 2008.

[7] G. Vasile, J.-P. Ovarlez, F. Pascal, and C. Tison. Coherency Matrix Estimation of Heterogeneous Clutter in High Resolution Polarimetric SAR Images. *IEEE Transactions on Geoscience and Remote Sensing*, 48(4):1809 – 1826, 2010.